# Hydrazine-assisted Liquid Exfoliation of $MoS_2$ for Catalytic Hydrodeoxygenation of 4-Methylphenol

Guoliang Liu,[a,b] Hualong Ma,[b] Ivo Teixeira,[a] Zhenyu Sun,[a] Qineng Xia,[a] Xinlin Hong,[b] and Shik Chi Edman Tsang*[a]

[a] G. Liu, I. Teixeira, Z. Sun, Q. Xia, Prof. S. C. E. Tsang*
Wolfson Catalysis Centre, Department of Chemistry
University of Oxford
Oxford, OX1 3QR (UK)
E-mail: edman.tsang@chem.ox.ac.uk

[b] G. Liu, H. Ma, Prof. X. Hong
Department of Chemistry
Wuhan University
Wuhan 430072, P.R. China

Supporting information for this article is given via a link at the end of the document.

**Abstract:** We present a simple but effective method to exfoliate bulk $MoS_2$ in a range of solvents for preparation of colloid flakes of mono to few molecular layers with application of ultrasonic treatment in $N_2H_4$: their high yield in solution with exposure of more active surface sites allows synthesis of corresponding solid catalysts with remarkably high activity in hydrodeoxygenation of 4-methylphenol and this method can also be applied to other two dimensional materials.

Layer-structured materials (LMs) have attracted enormous attention due to unusual properties of two-dimensional nanosheets.[1-3] In this big family, transition metal dichalcogenides (TMD) such as $MoS_2$, $WS_2$ are the one of the most important LMs.[4,5] It has recently been demonstrated that when the thickness of this structure is reduced to mono to few molecular layers, the nanosheets can show exceptional optical, electronic, magnetic and mechanical properties because of the change in band structure and hence affecting electron arrangement.[6] This may bring new prospective to different fields, including energy storage, smart electronic components, optical devices and catalysis.[7-16] However, the development of these new materials has been hampered by the lack of simple method to prepare mono- or few layer flakes in large quantities. Therefore, it would be of great technological significance to exfoliate bulk LMs in high yield by a simple technique to facilitate film production or spray deposition for various applications.

It is well known that the structure of TMDs consists of sandwiched X-M-X (X=S, Se, Te, M=Mo, W, Ti, etc.) molecular layers which are held by weak van der Waals interaction, similar to graphite. This weak interaction allows the preparation of 2-D nanosheets in solution through a number of top-down exfoliation methods of bulk crystals. Physical or mechanical cleavage by a scotch-tape method can be used to extract high quality mono- or few- layered TMDs,[17-19] but this method is difficult to scale up for mass production. Alkali-metal intercalation is another well accepted method for exfoliation.[20,21] Zhang's group employed a modified electrochemical lithiation method to facilitate higher yield production of single-layer TMDs.[22] However chemical method is synthetically cumbersome and the materials are highly sensitive to operating conditions. The removal of reactive intercalate(s) from solution often causes immediate re-aggregation of exfoliated layers. Furthermore, the intercalation and de-intercalation processes associated with electronic change also induce structural transformation of TMDs.

Recently a direct liquid exfoliation method with ultrasonic treatment is demonstrated to show enormous potentials in mass scale production to meet industrial requirements. Coleman and co-workers employed this method to exfoliate LMs to nanosheets efficiently in a selected solvent with appropriate Hansen solubility parameters.[23] Such physical separation method demonstrates an aesthetic appeal due to its simplicity and ease of handling without any chemical reaction involved. Importantly, highly dispersed LMs of reduced dimension in solution with intact intrinsic structure can be established for film manufacture for a wide range of potential applications. A great number of solvents were studied and amongst them, N-methyl-2-pyrrolidone (NMP) and other pyrrolidone-based solvents were found to be effective for the exfoliation of TMDs.[23-25] However, complete removal of these solvents was challenging due to their general high boiling point nature. On the other hand, the use of surfactant molecules is also capable of assisting liquid exfoliation, but the surfactant molecules are normally difficult to recycle.[26,27] Recently, mixed solvents of alcohol and water have been developed for efficient exfoliation of LMs.[28] A water-alcohol solvent mixture at optimal ratio can lead to higher yield. By determining liquid-solid interfacial energy, Halim and colleagues demonstrated an effective exfoliation of $MoS_2$ and graphite in isopropanol/water mixture with an optimal co-solvent concentration of 30 v/v%.[29] Despite the low cost and environmental friendly of the mixed solvents, the mixed alcohol-water systems still suffer from drawbacks such that the prepared dispersions are relatively low in LMs content, normally of lower than 0.1 mg ml$^{-1}$.[28]

Here, we demonstrate a new but simple method using hydrazine ($N_2H_4$) to assist the liquid exfoliation of bulk $MoS_2$ in 30 v/v% isopropanol-water mixture (IPA/W) with ultrasonic treatment. In our procedure, only a small amount of $N_2H_4$ (normally < 5 v/v%) is required and the yield of dispersed $MoS_2$ nanosheets can be greatly enhanced. The exfoliation efficiencies, in the cases of $MoS_2$ and graphene are clearly increased by more than three times than that without $N_2H_4$, giving the yield of material flakes in solution of 1.48 mg mL$^{-1}$. It is also shown that this new method is versatile and can be applicable to other 2D materials in dispersant systems, such as DMF and aqueous surfactant solutions. In addition, we show that the $MoS_2$ nano-sheets prepared by this method can be used as efficient catalysts which display excellent hydrodeoxygenation (HDO) activity with and without adding cobalt promoter.

The exfoliated $MoS_2$ suspension was prepared through sonication of bulk powder in IPA/W system with and without addition of 4 v/v% $N_2H_4$. Figure S1 in SI shows transition electron microscopy (TEM) and scanning electron microscopy (SEM) images of original bulk $MoS_2$ used. It is characterised with large aggregated multi-layered particles of lateral size varying from 500 nm to 2 μm. After exfoliation and centrifugation, colloidal suspensions in solution were obtained and the optical images are shown in Figure S2. Clearly, $N_2H_4$ treated samples are associated with more intense and darker colour solutions than those without $N_2H_4$ treatment, suggesting that a higher concentration of exfoliated nanosheets can be obtained under comparable conditions. The dispersions can be stable for at least several weeks. Also this method seems to be effective for the exfoliation of $WS_2$ and graphite (Figure S3).

Figure 1a shows the TEM image of a large $MoS_2$ nanosheet deposited on carbon grid. A great number of small flakes were formed after thinning and cracking of the crystals precursors (see Figure S4). They show rather irregular shape with lateral size ranging from 40 to 100 nm. From their images, we can see some flakes with substantial reduced thickness from mono- to few-layers. A d-spacing of 0.27 nm was observed of stacked fringes in the high resolution images (Figure S4c). This matches well with the characteristic (100) facets of hexagonal structure of $MoS_2$, indicating a top view through c-axis direction. Additionally, the enlarged image shown in Figure 1b clearly illustrates the hexagonal lattices of $MoS_2$, which are consistent with the 2H-structure.[20] We employed atomic force microscopy (AFM) to measure the average thickness of the exfoliated $MoS_2$. Figure 1c shows the typical step height of around 2.5 nm, which is approximately two to three times than that of a single molecular layer within experimental errors of this technique.[20,29] The statistical analysis of flake thickness was then carried out from AFM images carefully over 92 flakes. As seen in Figure 1d, the thickness can be ranged from 1-10 nm, with an average of 3.7 nm, suggesting the formation of small flakes of reduced thickness from mono- to few-layered $MoS_2$ as compared to the bulk counterpart. Raman spectra in Figure S5 show that both the out-of-plane $A_{1g}$ and in-plane $E^1_{2g}$ vibrations soften (red shift by around 3 $cm^{-1}$) after exfoliation, in good agreement with those of exfoliated few layers reported by Coleman et al.[30] The quality of these reduced LMs layers seems to be comparable to those prepared by typical liquid exfoliation routes.[23-30]

UV-vis spectroscopy was used to estimate exfoliation efficiency since exfoliated $MoS_2$ forms stable colloidal suspension in solution even after centrifugation to remove non-exfoliated sediment.[26] By subtracting the scattering background, the absorbance value is in a linear function of $MoS_2$ concentration based on the Lambert–Beer law ($A/l = \varepsilon C$, where A /l is the absorbance per cell length, ε the absorption coefficient, *C* the dispersed concentration). Typically, the absorption of $MoS_2$ suspension shown in Figure S6 displays four characteristic absorption peaks.[31] The peaks A and B at 670 and 608 nm respectively, can be assigned to the smallest direct transitions (band edge excitons) in 2H-$MoS_2$, while peaks at 454 and 397 nm originate from interband transitions from occupied $dz^2$ orbital to unoccupied dxy, $x^2$-$y^2$ and dxz, yz orbitals.[32] The absorbance value of peak A was used to estimate exfoliation yield with and without the addition of $N_2H_4$. Similarly, absorbance at 632 and 265 nm were used to estimate the exfoliation efficiencies in the cases of $WS_2$ and graphene, respectively (see Figure S6).

Figure 2a demonstrates clearly that the absorbance values are significantly enhanced for all the three layered materials after the addition of $N_2H_4$ under identical amounts of sample and solvent and 2 h sonication treatments, namely, 2.4 folds for $MoS_2$, 1.5 folds for $WS_2$ and 3.3 folds for graphene. Regarding the effects of sonication time and $N_2H_4$ concentration, Figure 2b shows that the absorbance of $MoS_2$ progressively increases with these two parameters. Interestingly, the exfoliation efficiency is only slightly affected by the $N_2H_4$ concentration at short time indicative of a slow diffusion of the molecules into the layered structure, however, at longer sonication duration of over 3-5h, lower concentration appears to be more effective for the exfoliation (1% $N_2H_4$ > 2% $N_2H_4$ > 4% $N_2H_4$). Similarly, in the case of graphene (Figure 2c), there appears to show an optimal concentration of $N_2H_4$ (0.4%) whereas higher concentration (1% $N_2H_4$) in fact gives lower absorbance. By studying three different solvent systems with very different solvent properties, namely IPA/W, dimethylformamide (DMF) and sodium dodecyl sulfate aqueous solution (SDS/W) in 1 v/v% $N_2H_4$ (Figure 2d), the absorbances are all increased but $N_2H_4$-IPA/W mixture shows the best exfoliation performance.

The simple method may be adopted for large-scale production of exfoliated materials (Figure S7). In our typical preparation of 12-h sonication, 1.04 g of exfoliated powder was collected from 0.7 L of solvent mixture, giving the exfoliated $MoS_2$ yield of 1.48 mg $mL^{-1}$. As far as we are aware, this value currently in alcohol/water mixed system is favourable in comparison with recent reported exfoliation methods, such as 0.8 mg $mL^{-1}$ with LiOH in NMP[24], 0.5 mg $mL^{-1}$ in aqueous sodium cholate[26] and 0.8 mg $mL^{-1}$ in aqueous SDS combined with ball milling[27], etc. At present, the mechanism for significant enhanced yield in such dilute $N_2H_4$ is not yet known. However, nitrogen containing molecules have been generally used as molecular intercalators for LMs, especially the TMDs because the lone-pair of nitrogen can form Lewis acid-base bonding with partially filled transition metal chalcogenide orbitals by electron charge transfer mechanism.[33] For example, a report was found using intercalation and de-intercalation of $MoS_2$ with $NH_3$ to assist exfoliation.[34] $N_2H_4$ molecules were reported to be effective to intercalate to $TiS_2$, $TiSe_2$ and $ZrS_2$ layered materials.[35] $N_2H_4$ is also known to intercalate many other layered materials as well, for example, clays[36] or carbides[37]. As a result, apart from the larger solvent molecules, we anticipate that the smaller size $N_2H_4$ molecules would also intercalate into TMD structures alongside with the solvent molecules as either neutral $N_2H_4$ or protonated $N_2H_5^+$ during sonication. Although there is no evidence on functionalization of these LM sheets on edge or defect regions as XPS indicated no significant content of nitrogen in our dried powder was detected (refer to Figure S8 for survey scans), we cannot directly rule out its possibility. It is well accepted that ultrasonic treatment in solvent can create 'cavitation' by energetic standing wave in miniscule region leading to the radicals formation from the solvent: in water, OH* and H* would be preferentially formed.[38] They will react with chemical attached or intercalated $N_2H_4$ to generate $N_2$ and $H_2O$ between the trapped molecular layers. Apparently, the sudden expansion in volume due to ultrasonic cavitation and reactions could thus assist the exfoliation process.

To support this postulation, top gas above the $N_2H_4$ treated solution during exfoliation was collected and then analysed using gas chromatography. The gas composition is shown in Table S1. It is interesting to reveal that $O_2$ was indeed largely consumed, along with evolution of $N_2$ and a trace of $H_2$. This observation agrees with the reported sonochemical degradation mechanism of $N_2H_4$ in waste water.[39] Thus, the reactions in localized cavitation would cause rapid gasification of intercalated $N_2H_4$/$N_2H_5^+$ to $N_2$, $H_2$, $H_2O$ or $NH_3$ between the molecular layers, leading to more effective exfoliation of TMDs. Intuitively, we anticipate that excess $N_2H_4$ molecules in solvent would also consume the limited amount of radicals generated during ultrasonic treatment hence protecting the intercalated $N_2H_4$ molecules from destruction. As a result, the use of higher $N_2H_4$ concentration was found to be less effective on the exfoliation yield (see Figs. 2b and c).

It is important to assess the quality of exfoliated nanosheets and explore their potential uses. We thus examined the $MoS_2$ nanosheets prepared by this method. Figure S8 (SI) shows the XPS spectra of Mo 3d peaks of exfoliated MoS2. They can be assigned to $Mo^{4+}$ $3d_{3/2}$ (232.9 eV) and $Mo^{4+}$ $3d_{5/2}$ (229.7 eV) with the same positions as those of 2H bulk crystals. Also, the single doublet peak of S corresponding to $2p_{1/2}$(163.8 eV) and $2p_{3/2}$(162.7 eV) is consistent with that of $S^{2-}$ in 2H $MoS_2$.[20] Figure S9 (SI) shows electron paramagnetic resonance (EPR) spectra of $MoS_2$ with and without exfoliation, which can quantify the trapped radicals due to the creation of sulphur vacancies.[40] Notice from the figure, after exfoliation, the signal at g=2.0 becomes intensified, indicating the concentration of sulphur vacancies increases to $5.44\times10^{17}$ counts $g^{-1}$ from the bulk value of $1.41\times10^{17}$ counts $g^{-1}$ (3.8 times). Interestingly, BET analysis also indicated a surface area increase by about 3 times (25.0 $m^2$ $g^{-1}$ for exfoliated sample, 8.4 $m^2$ $g^{-1}$ for the bulk as shown in Figure S10). This clearly suggests that the newly generated surfaces from exfoliation of bulk $MoS_2$ material contain similar amounts of intrinsic defects per surface area per gram without creating much additional vacancies or structural damages. Interestingly, for the exfoliation of graphite, the few layered graphene obtained in $N_2H_4$ containing system actually shows a slightly lesser amount of defects than that without $N_2H_4$, as the characteristic $I_D/I_G$ ratio decreases from 0.47 to 0.37 in Raman spectra (Figure

S11).[41] This reinforces the fact that $N_2H_4$ consumes radicals under strong ultrasonic treatment from their structural damage to the graphene.[42] Thus this method can retain the structural and electronic integrities of the LMs structures, which is clearly advantageous over to the alkali intercalation methods that cause a structural transition from 2H to 1T phase with a significant enhancement of sulphur vacancies per gram or per surface area basis.[20]

$MoS_2$ is a well-known catalyst component in hydrodesulfuration (HDS) and hydro-deoxygenation (HDO) reactions, which represents a major industrial use of this transition metal chalcogenide.[43] So far, there are very few reports in open literature concerning the catalytic performance of using exfoliated $MoS_2$ for the HDO reactions.[44] However, the access of higher surface area of ultrathin $MoS_2$ flakes prepared by this method with and without support (on high surface supported material to host the MoS2 nanosheets) is attractive in this catalyst preparation. Nevertheless, one concern is that according to the classical "rim-edge" theory[45], the decrease in stacking of $MoS_2$ could result in the increase in rim to edge atoms ratio and thereby promoting undesirable hydrogenation (HYD) by the rim atoms, rather than hydro-de-oxygenation route by the edge atoms. We tested our exfoliated $MoS_2$ as catalyst in HDO of 4-methylphenol (Table 1). It is noted that $MoS_2$ after exfoliation indeed becomes more active, giving a higher conversion of 69.6% as compared to bulk $MoS_2$ (25.8%) due to enhanced surface area. The kinetic analysis suggests that the reaction is apparent first order dependence with a rate constant of 0.168 as compared to 0.029 in bulk $MoS_2$ (Figure S12). Although the desirable hydro-deoxygenation product, the toluene is still mainly produced, the exfoliated nanosheets indeed show a lower toluene selectivity of 87.2% as compared to bulk $MoS_2$ (94.0%) in favour of other hydrogenation products.

Cobalt promotion to the $MoS_2$ flakes was also synthesised, which is known to enhance catalytic activity for HDO and HDS reactions.[43] Taking the advantage of colloidal stable exfoliated $MoS_2$, a simple mixing with a soluble Co precursor (cobalt acetate), followed by reduction and flocculation using $NaBH_4$ (see experimental section in SI). After air exposure, the TEM images of the sample displayed in Figure 3 show the presence of extremely small Co containing nanoparticles (about 2 nm) which are homogeneously distributed on the basal surfaces of $MoS_2$ at high coverage. Under closer examination of the images, it is found that a higher degree of Co deposition had been particularly taken place on the rim/edge region. A lattice spacing of 0.21 and 0.25 nm, assigned to (200) and (111) of cubic CoO[46] can be visualized from these small particles (Figure S13), presumably they were formed after the air oxidation of corresponding Co metal nanoparticles. XPS data also indicated the presence of $Co^{II}$ species and the EDX analysis gave Co/Mo atom ratio of 0.3. Table 1 shows that the activity and selectivity over the Co promoted $MoS_2$ flakes prepared with the $N_2H_4$ treatment are dramatically increased. The high activity of HDO reaction of 4-methylphenol over Co-$MoS_2$ flakes, with low HYD/HDO ratio of 0.045 is attributed partly to the activated $MoS_2$ sites at the interface with Co atoms due to their lower enthalpies of both $H_2$ and oxygenated compound co-activations[47] and partly to the selective blockage of the rim sites by Co. The use of mono- or few molecular layers as hosts for reactive atoms or clusters apparently enables molecular design of superior catalysts and their deposition.

In summary, we present a simple, facile but effective method to exfoliate $MoS_2$, graphene, $WS_2$ and related LMs in dilute hydrazine to yield mono- and few-layer nanosheets in IPA/water system with ultrasonic treatment. A small amount of $N_2H_4$ can greatly facilitate the exfoliation process. This method can be adopted for mass production and can be applicable to different solvent systems. During exfoliation, $N_2H_4$ molecules are thought to intercalate to molecular layers of LMs structure under ultrasonic treatment and rapid radicals reactions to $N_2$ and $H_2O$ by cavitation enables effective exfoliation. As a result, the $MoS_2$ nanosheets prepared from bulk form by this simple method are shown to generate more active surface for cobalt promotion, which give superior catalytic performance in HDO.

## Experimental Section

All chemicals used were purchased from Sigma-Aldrich and used without further purification or modification. Typically, powder $MoS_2$, graphite or $WS_2$ (25 mg) was dispersed into 30 v/v% IPA/W, 1.5 mg mL$^{-1}$ SDS/W or DMF (5 mL), making initial concentration equal to 5 mg/mL. Then an appropriate amount (see details in main text) of hydrazine monohydrate was added into the mixed system, followed by a sonication process in a sonic bath. The samples were placed in different positions in sonic bath in every ten-minute cycle to give uniform sonication distribution. After that, the resulting suspensions were centrifuged at 7000 rpm for 15 minute and upper supernatant was then collected by pipette followed by another centrifugation at 7000 rpm for 10 minute to further remove non-exfoliated sediment. The absorbance of exfoliated $MoS_2$, $WS_2$ and graphene dispersions was taken at 670, 632 and 265 nm, respectively. Then, the values were used to evaluate the exfoliation efficiency. The large-scale production of exfoliated $MoS_2$, preparation of Co-$MoS_2$ composite, conditions for hydrodeoxygenation reaction and product analyses can be found in Supporting Information.

## Acknowledgements

The authors are grateful to the CSC to grant studentship to G. Liu and Q. Xia to work at Oxford.

## References

[1] K. S. Novoselov, A. K., Geim, S. V. Morozov, D. Jiang, Y. Zhang, S. V. Dubonos, I. V. Grigorieva, A. A. Firsov, *Science* **2004**, *306*, 666−669.
[2] A. K. Geim, K. S. Novoselov, *Nat. Mater.* **2007**, *6*, 183−191.
[3] H. Zhang, *ACS Nano* **2015**, *9*, 9451-9469.

[4] A. K. Geim, I. V. Grigorieva, *Nature* **2013**, *499*, 419-425.

[5] H. Li, J. Wu, Z. Yin, H. Zhang, *Acc. Chem. Res.* **2014**, *47*, 1067-1075.

[6] K. F. Mak, C. Lee, J. Hone, J. Shan, T. F. Heinz, *Phys. Rev. Lett.* **2010**, *105*, 136805(4).

[7] T. Stephenson, Z. Li, B. Olsenab, D. Mitlin, *Energy Environ. Sci.* **2014**, *7*, 209–231.

[8] Y. Li, H. Wang, L. Xie, Y. Liang, G. Hong, H. Dai, *J. Am. Chem. Soc.* **2011**, *133*, 7296−7299.

[9] D. J. Late, B. Liu, H. S. S. R. Matte, V. Dravid, C. N. R. Rao, *ACS Nano* **2012**, *6*, 5635−5641.

[10] B. Radisavljevic, A. Radenovic, J. Brivio, V., Giacometti, A. Kis, *Nat. Nanotechnol.* **2011**, *6*, 147−150.

[11] M.-L. Tsai, S.-H. Su, J.-K. Chang, D.-S. Tsai, C.-H. Chen, C.-I Wu, L.-J. Li, L.-J. Chen, J.-H. He, *ACS Nano* **2014**, *8*, 8317–8322.

[12] C. Tan, H. Zhang, *J. Am. Chem. Soc.* **2015**, *137*, 12162-12174.

[13] C. Tan, H. Zhang, *Chem. Soc. Rev.* **2015**, *44*, 2713-2731.

[14] C. Tan, Z. Liu, W. Huang, H. Zhang, *Chem. Soc. Rev.* **2015**, *44*, 2615-2628.

[15] X. Huang, Z. Zeng, H. Zhang, *Chem. Soc. Rev.* **2013**, *42*, 1934-1946.

[16] X. Huang, C. Tan, Z. Yin, H. Zhang, *Adv. Mater.* **2014**, *26*, 2185-2204.

[17] Z. Yin, H. Li, H. Li, L. Jiang, Y. Shi, Y. Sun, G. Lu, Q. Zhang, X. Chen, H. Zhang, *ACS Nano* **2012**, *6*, 74–80.

[18] H. Li, G. Lu, Z. Yin, Q. He, H. Li, Q. Zhang, H. Zhang, *Small* **2012**, *8*, 682-686.

[19] H. Li, G. Lu, Y. Wang, Z. Yin, C. Cong, Q. He, L. Wang, F. Ding, T. Yu, H. Zhang, *Small* **2013**, *9*, 1974-1981.

[20] G. Eda, H. Yamaguchi, D. Voiry, T. Fujita, M. Chen, M. Chhowalla, *Nano Lett.* **2011**, *11*, 5111−5116.

[21] J. Zheng, H. Zhang, S. Dong, Y. Liu, C. T. Nai, H. S. Shin, H. Y. Jeong, B. Liu, K. P. Loh, *Nat. Commun.* **2014**, *5*, 2995.

[22] Z. Zeng, Z. Yin, X. Huang, H. Li, Q. He, G. Lu, F. Boey, H. Zhang, *Angew. Chem. Int. Ed.* **2011**, *50*, 11093-11097.

[23] J. N. Coleman , M. Lotya, A. O'Neill , S. D. Bergin, P. J. King, U. Khan, K. Young, A. Gaucher, S. De , R. J. Smith, I. V. Shvets, S. K. Arora, G. Stanton , H. Y. Kim, K. Lee, G. T. Kim, G. S. Duesberg, T. Hallam, J. J. Boland, J. J. Wang, J. F. Donegan, J. C. Grunlan , G. Moriarty, A. Shmeliov, R. J. Nicholls, J. M. Perkins, E. M. Grieveson, K. Theuwissen, D. W. McComb, P. D. Nellist, V. Nicolosi, *Science* **2011**, *331* , 568.

[24] G. S. Bang, K. W. Nam, J. Y. Kim, J. Shin, J. W. Choi, S.-Y. Choi, *ACS Appl. Mater. Interfaces* **2014**, *6*, 7084−7089.

[25] A. O'Neill, U. Khan, J. N. Coleman, *Chem. Mater.* **2012**, *24*, 2414-2421.

[26] R. J. Smith, P. J. King, M. Lotya, C. Wirtz, U. Khan, S. De, A. O'Neill, G. S. Duesberg, J. C. Grunlan, G. Moriarty, J. Chen, J. Wang, A. I. Minett, V. Nicolosi, J. N. Coleman, *Adv. Mater* **2011**, *23*, 3944–3948.

[27] Y. Yao, Z. Lin, Z. Li, X. Song, K.-S. Moon, C. Wong, *J. Mater. Chem.* **2012**, *22*, 13494–13499.

[28] K.-G. Zhou, N.-N. Mao, H.-X. Wang, Y. Peng, H.-L. Zhang, *Angew. Chem., Int. Ed.* **2011**, *50*, 10839–10842.

[29] U. Halim, C. R. Zheng, Y. Chen, Z. Lin, S. Jiang, R. Cheng, Y. Huang, X. Duan, *Nat. Commun.* **2013**, *4*, 2213.

[30] G. Cunningham, M. Lotya, C. S. Cucinotta, S. Sanvito, S. D. Bergin, R. Menzel, M. S. P. Shaffer, J. N. Coleman, *ACS NANO* **2012**, *6*, 3468-3480.

[31] L. A. King, W. Zhao, M. Chhowalla, D. J. Rileya, G. Eda, *J. Mater. Chem. A* **2013**, *1*, 8935–8941.

[32] R. Coehoorn, C. Haas, J. Dijkstra, C. J. F. Flipse, *Phys. Rev. B: Condens. Matter Mater. Phys.* **1987**, *35*, 6195–6202.

[33] F. R. Gamble and B. G. Silbernagel, *J. Chem. Phys.***1975**, *63*, 2544.

[34] A. A. Jeffery, C. N. Nethravathi, M. Rajamathi, *J. Phys. Chem. C* **2014**, *118*, 1386-1396.

[35] A. M. Ghorayeb, R. H. Friend, J. Phys. C: Solid State Phys. **1987**, *20*, 4181-4200.

[36] Y. Deng, J. B. Dixon, G. N. White, *J. Colloid Interface Sci.* **2003**, *257*, 208-227.

[37] O. Mashtalir, M. Naguib, V. N. Mochalin, Y. Dall'Agnese, M. Heon, M. W. Barsoum, Y. Gogotsi, *Nat. Commun.* **2013**, *4*, 1716.

[38] A. Weissler, *J. Am. Chem. Soc.* **1959**, *81*, 1077-1081.

[39] H. Nakui, K. Okitsu, Y. Maeda, R. Nishimura, *Ultrasonics Sonochemistry* **2007**, *14*, 627-632.

[40] L. Cai, J. He, Q. Liu, T. Yao, L. Chen, W. Yan, F. Hu, Y. Jiang, Y. Zhao, T. Hu, Z. Sun, S. Wei, *J. Am. Chem. Soc.* **2015**, *137*, 2622–2627.

[41] M. A. Pimenta, G. Dresselhaus, M. S. Dresselhaus, L. G. Cancado, A. Jorio, R. Saito, *Phys. Chem. Chem. Phys.* **2007**, *9*, 1276–1291.

[42] K. S. Rao, J. Senthilnathan, Y.-F. Liu, M. Yoshimura, *Sci. Rep*, **2014**, *4*, 4237.

[43] M. Saidi, F. Samimi, D. Karimipourfard, T. Nimmanwudipong, B. C. Gates, M. R. Rahimpour, *Energy Environ. Sci.* **2014**, *7*, 103–129.

[44] Y. Q. Yang, C. T. Tye, K. J. Smith, *Catal. Commun.* **2008**, *9*, 1364-1368.

[45] M. Daage, R.R. Chianelli, *J. Catal.* **1994**, *149*, 414–427.

[46] W. S. Seo, J. H. Shim, S. J. Oh, E. K. Lee, N. H. Hur, J. T. Park, *J. Am. Chem. Soc.* **2005**, *127*, 6188-6189.

[47] F. Y. Cheng, J. Chen, X. L. Gou, *Adv. Mater.* **2006**, *18*, 2561-2564.

Scheme and Figure legends

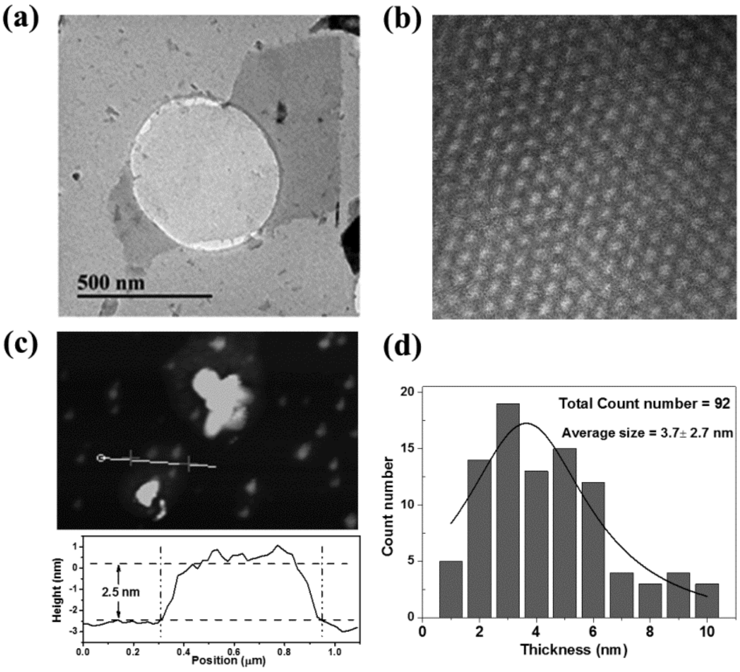

**Figure 1.** (a) A TEM image of exfoliated $MoS_2$ flake prepared in IPA/W mixed solvents with $N_2H_4$ treatment; (b) enlarged HRTEM image showing 2-H structure of $MoS_2$ (c) AFM image (above) and a line scan of a $MoS_2$ sheet (below); (d) statistic thickness distribution of exfoliated $MoS_2$ flakes.

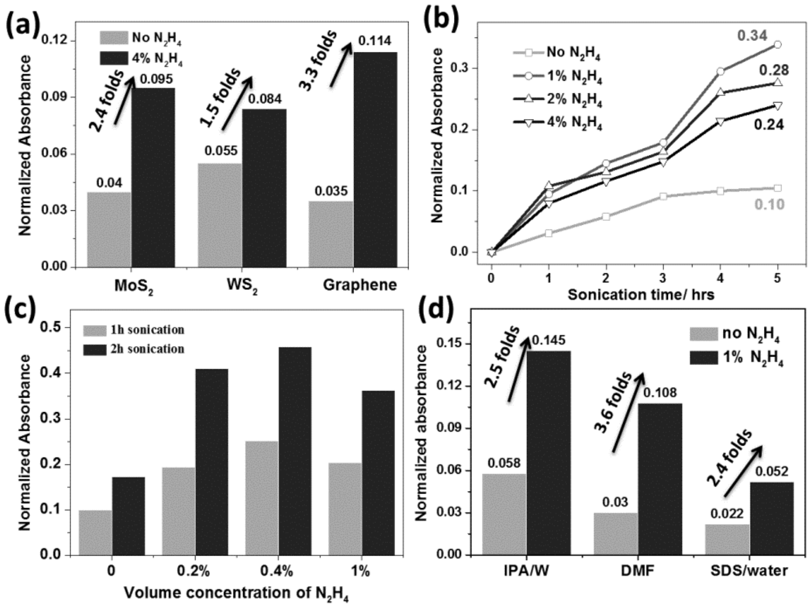

**Figure 2.** Absorbance of exfoliated (a) $MoS_2$, $WS_2$ and graphene in IPA/W over 2-h sonication with and without addition of 4% $N_2H_4$, (b) For $MoS_2$, the change in absorbance as a function of sonication time in IPA/W with different concentration of $N_2H_4$, (c) For graphene, the change in absorbance in different concentration of $N_2H_4$, and (d) For $MoS_2$, the use of different solvent: IPA/W, DMF and SDS/Water over 2-h sonication with and without 1% $N_2H_4$.

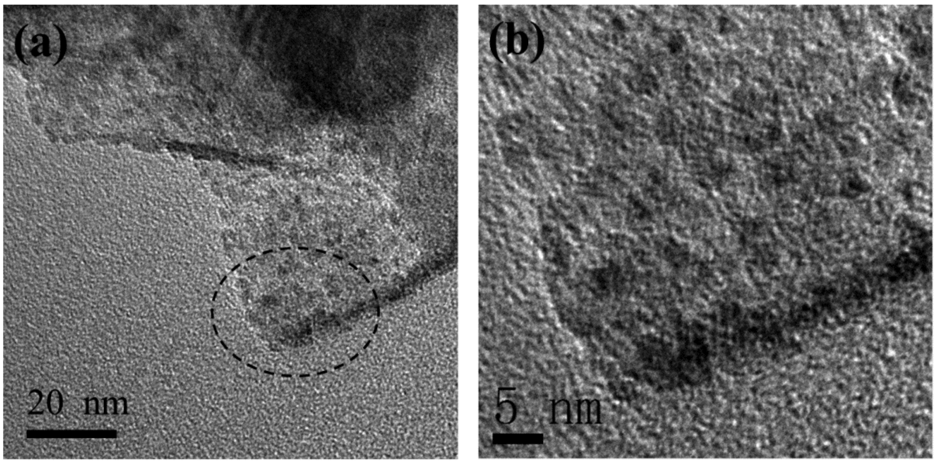

**Figure 3.** (a) A TEM image of Co doped $MoS_2$ flakes showing 2 nm Co containing nanoparticles are rather homogeneously deposited on flat $MoS_2$ nano-sheets (b) Enlarged area HRTEM (dotted circle) shows a higher degree of deposition of Co containing nanoparticles on the rim of the nano-sheet.

# Tables

**Table 1.** Conversion and product selectivity in the HDO of 4-methylphenol over bulk, exfoliated and Co promoted $MoS_2$ catalysts.[a]

| Catalysts | Bulk $MoS_2$ | exfoliated $MoS_2$ | Co-$MoS_2$ |
|---|---|---|---|
| Conversion | 25.8% | 69.6% | 97.1% |
| Selectivity | | | |
| Toluene | 94.0% | 87.2% | 95.7% |
| Methylcyclohexane | 2.2% | 2.9% | 3.3% |
| 4-Methylcyclohexene | 0 | 4.0% | 0 |
| 1-Methylcyclohexene | 3.8% | 5.9% | 1.0% |
| HYD/HDO [b] | 0.064 | 0.147 | 0.045 |

[a] Reaction conditions: 300 °C, 3 MPa initial $H_2$ pressure, 6 h. [b] HYD/HDO= (1-Toluene selectivity)/Toluene selectivity.

## Text for the Table of Content

We present a simple but effective method to exfoliate bulk $MoS_2$ in a range of solvents for preparation of colloid flakes of mono to few molecular layers with application of ultrasonic treatment in $N_2H_4$: their high yield in solution with exposure of more active surface sites allows synthesis of corresponding solid catalysts with remarkably high activity in hydrodeoxygenation of 4-methylphenol and this method can also be applied to other two dimensional materials.

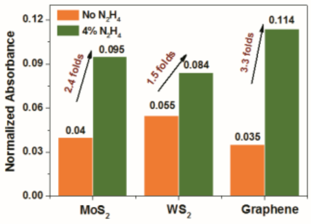

## Keywords

hydrazine • exfoliation • molybdenum disulphide • large-scale production • hydrodeoxygenation